The jet detections in radio-loud narrow-line Seyfert 1 galaxies

(Gu et al. 2015, ApJS, 221, 3; Gu et al. 2016, AN)

Minfeng Gu (SHAO)

Collaborators: Zhiqiang Shen, Yongjun Chen (SHAO); Weimin Yuan (NAOC); S. Komossa, J. A. Zensus (MPIfR); Hongyan Zhou (USTC); K. Wajima (KASI)

2016-10-19, Kathmandu

Shining from the heart of darkness: Black hole accretion and jets

Outline

- Introduction

  radio-loud AGNs

  narrow line Seyfert 1 galaxies (NLS1s)

- The radio structure of radio-loud NLS1s

  VLBA observations

  comparison with other AGNs

  scenarios

- Ongoing and future work
- Summary

AGN structure and radio-loud AGNs

- Radio loudness: $R \equiv L_{\nu 5\ \mathrm{GHz}} / L_{\nu 4400}$,

R>10 radio-loud; <1 radio-quiet;
1<R<10 radio intermediate
(Kellermann et al. 1994)

- Radio luminosity: $P_{6\ \mathrm{cm}} \approx 10^{25}\ \mathrm{W\,Hz^{-1}\,sr^{-1}}$ (Miller et al. 1990)

Only 10%–20% were qualified as radio-loud objects in optically selected samples (e.g., Kellermann et al. 1989; Hooper et al. 1995).

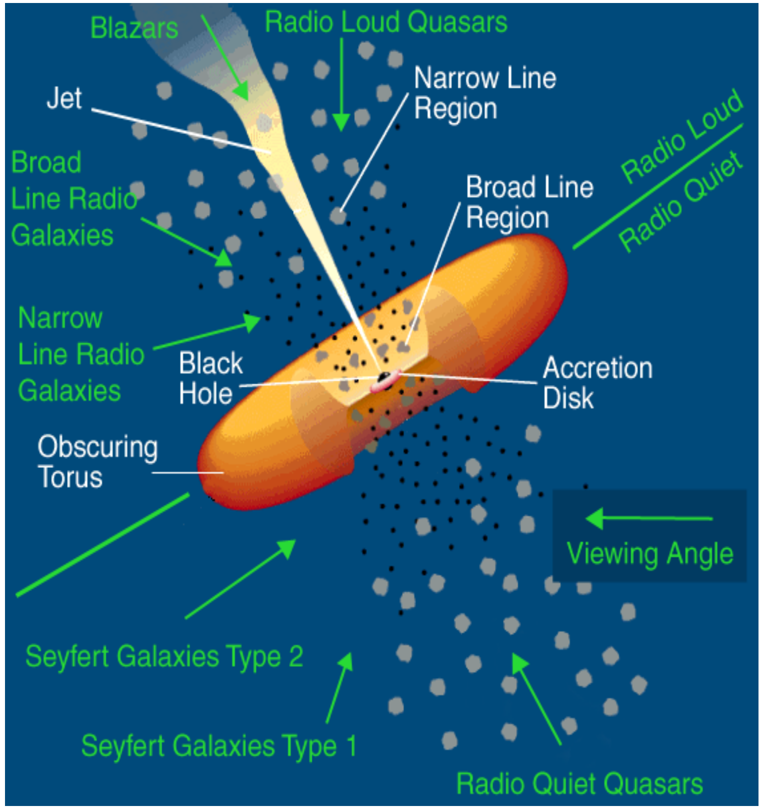

Urry & Padovani (1995)

Narrow Line Seyfert 1 galaxies (NLS1s)

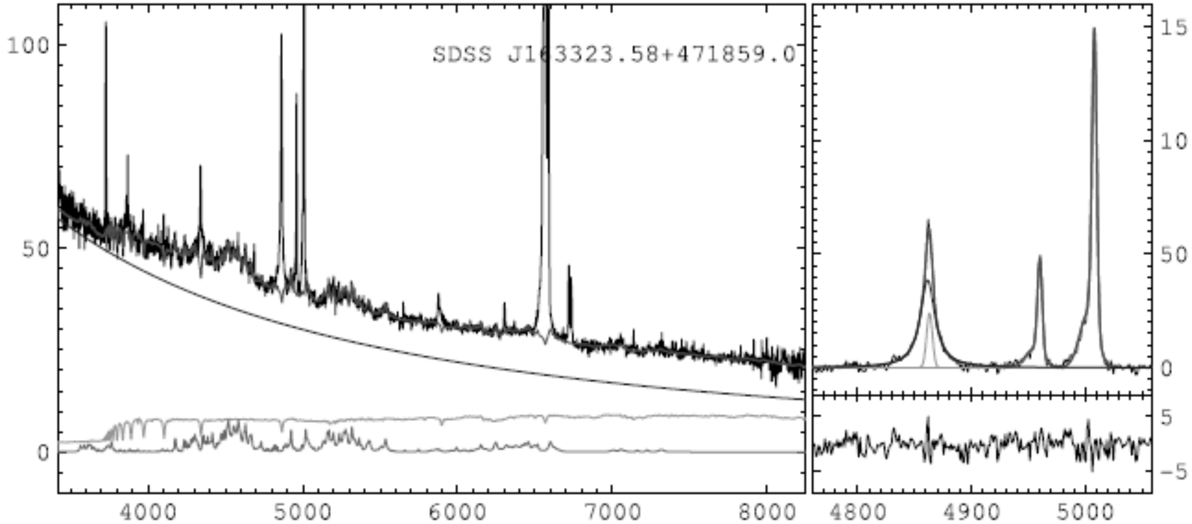

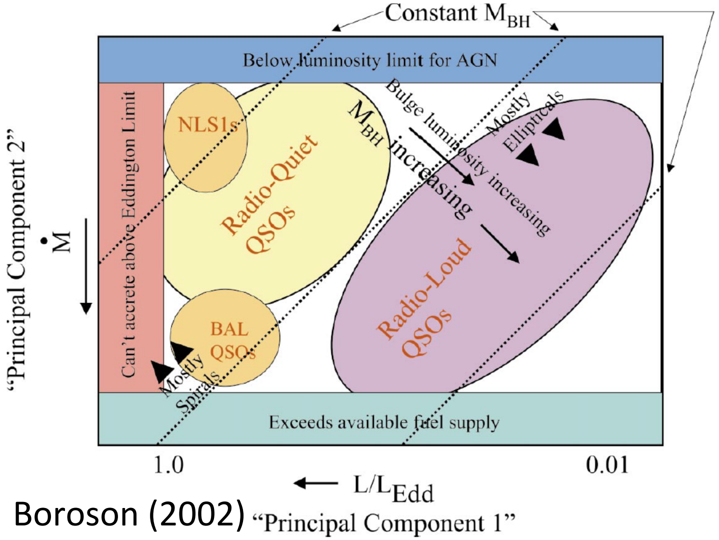

Boroson (2002)

FIG. 7.—Interpretive diagram showing how PC1-PC2 plane provides basis for classification of AGNs

- Balmer lines broader than forbidden lines but narrower than normal type 1 AGNs (FWHM < 2000km/s)
- Peculiar properties: softer X-ray spectra, fast X-ray variability, strong optical Fe IIs
- Relatively small black hole mass 10^{6-8} $M_{\odot}$(e.g. Collin & Kawaguchi 2004), however still controversial: viewing angle, radiation pressure …
- High accretion rate Lbol >> 0.1 L_{Edd} (up to Lbol/Ledd ~ 1)
- Accretion possible via slim disk (e.g. Abramowicz et al. 1988; Mineshige et al. 2000)

Radio-loud NLS1s (RLNLS1s)

- NLS1s were long thought to be radio-quiet. Radio-loud NLS1s are rare, but they do exist (Siebert et al 1999 ; Grupe et al. 2000; Zhou & Wang 2002; Zhou et al. 2003; Whalen et al. 2006; Komossa et al. 2006; Yuan et al. 2008).
- RL NLS1s sample from SDSS: >100 out of ~2000 NLS1s (Zhou et al. 2006) – RL (R>10) fraction = 7%; very radio-loud (R>100) NLS1s: very rare – 23 from SDSS DR5 (Yuan et al. 2008).

- Komossa et al. (2006): the radio loud NLS1 galaxies are generally compact, steep spectrum sources.

- Several of the radio loudest NLS1 galaxies display blazar characteristics and harbor relativistic jets (Doi et al. 2007; Zhou et al. 2007; Yuan et al. 2008)
- Flat radio spectra, large-amplitude flux and spectral variability, compact radio cores, very high variability brightness temperatures, enhanced optical continuum emission, flat X-ray spectra, and blazar-like SEDs.

Compact at arcsec scale

- Arcsecond-resolution observations have resolved the structures of only a few NLS1s because they are generally quite compact (e.g. Ulvestad et al. 1995, Moran et al. 2000, Stepanian et al. 2003, Doi et al. 2012).

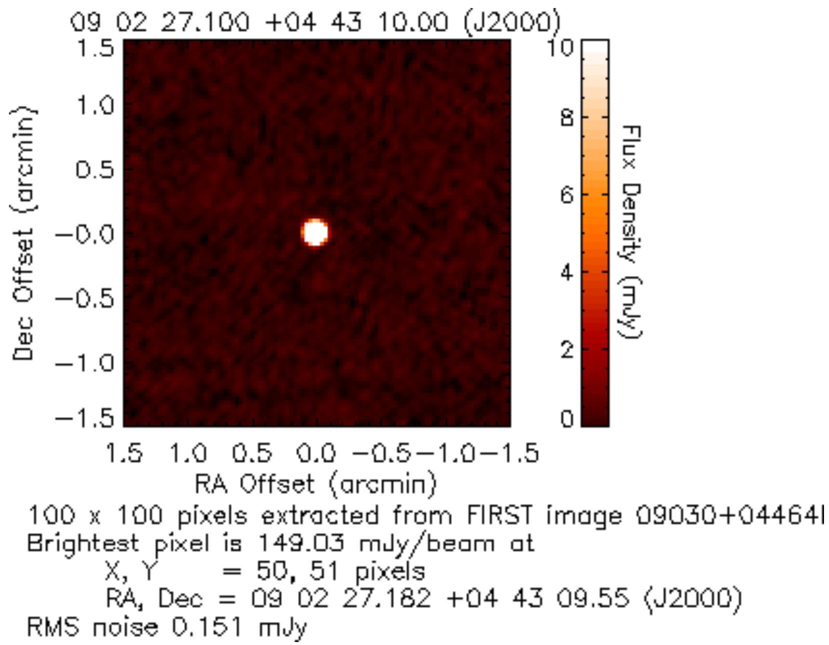

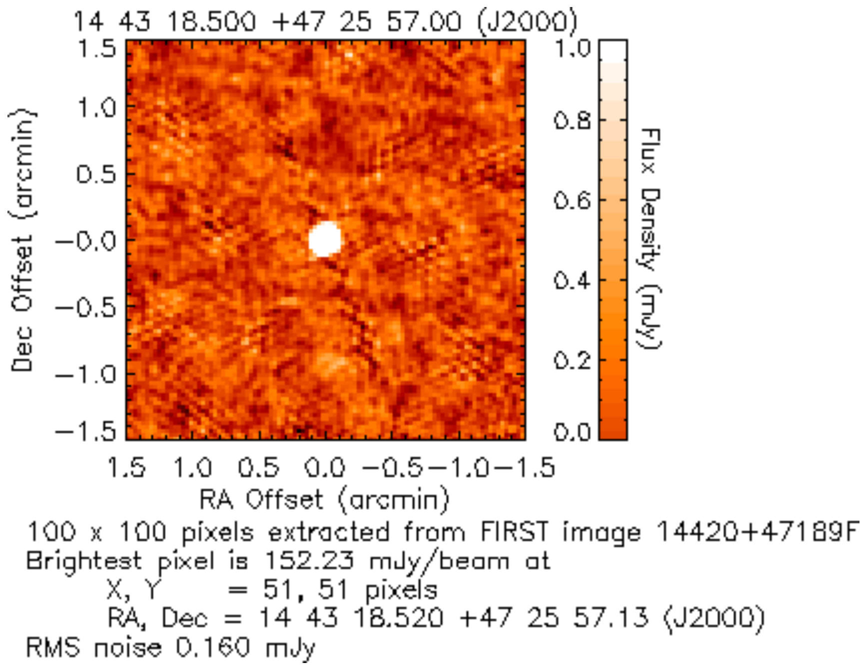

Host galaxies

- Almost all the low redshift NLS1s are hosted by spiral galaxies (Crenshaw et al. 2003, Deo et al. 2006)

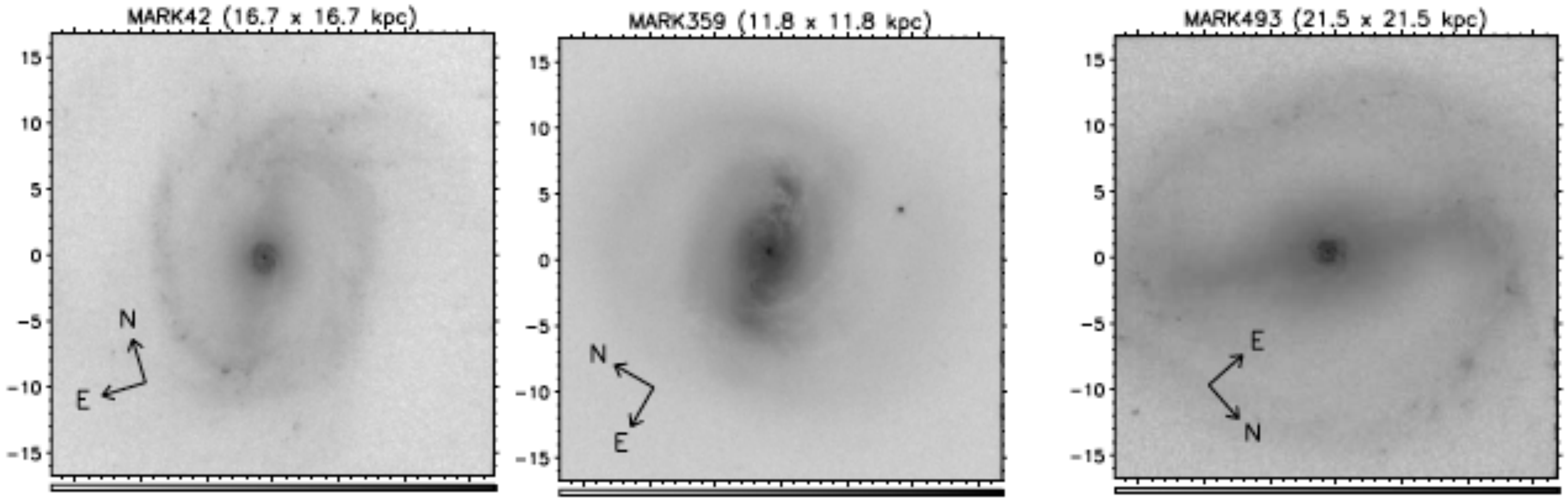

Host galaxies of RLNLS1s : unclear

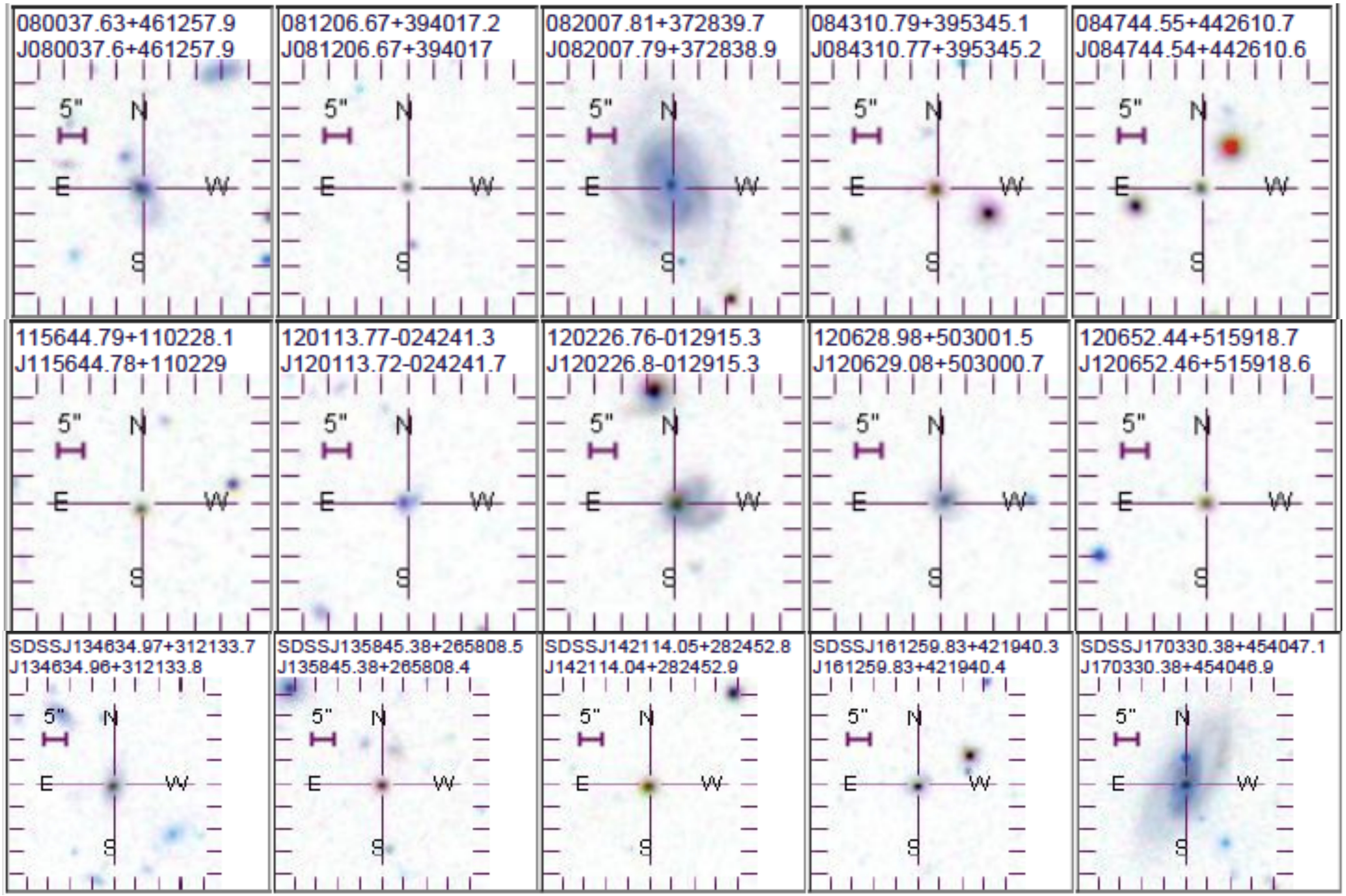

RLNLS1s in overall AGNs

- Relatively smaller M_{BH}, and larger accretion rate.
- Two sequences on R - Eddington ratio plane (Sikora et al. 2007).

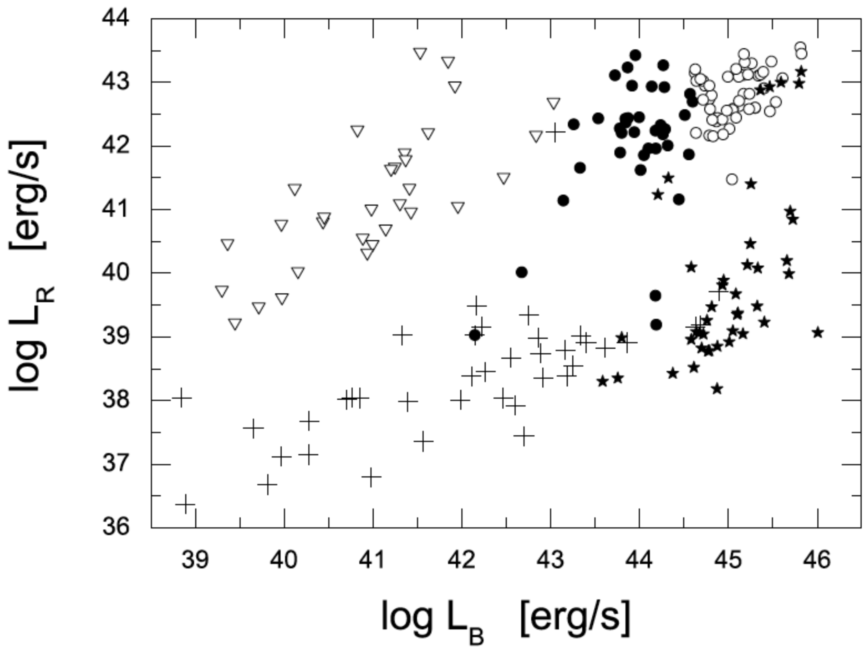

FIG. 1.—Total 5 GHz luminosity vs. *B*-band nuclear luminosity. BLRGs are marked by filled circles, radio-loud quasars by open circles, Seyfert galaxies, and LINERs by crosses, FR I radio galaxies by open triangles, and PG quasars by filled stars.

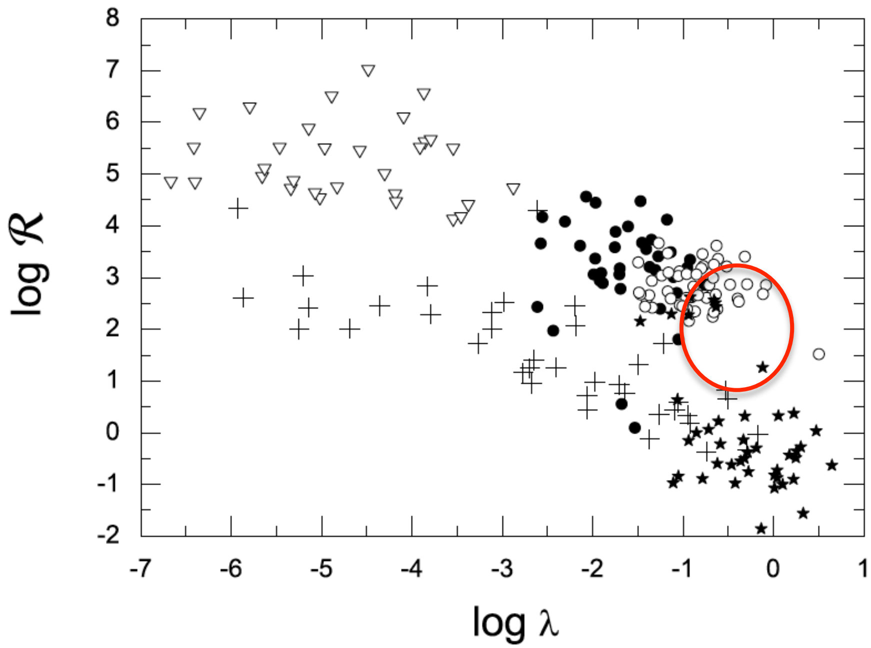

FIG. 3.—Radio loudness $\mathcal{R}$ vs. Eddington ratio λ. BLRGs are marked by filled circles, radio loud quasars by open circles, Seyfert galaxies and LINERs by crosses, FR I radio galaxies by open triangles, and PG quasars by filled stars.

Jet formation

- Jets in BHBs and AGNs: similar ?
- Jet-production related parameters: black hole mass, spin, host galaxy, accretion rate, environments …

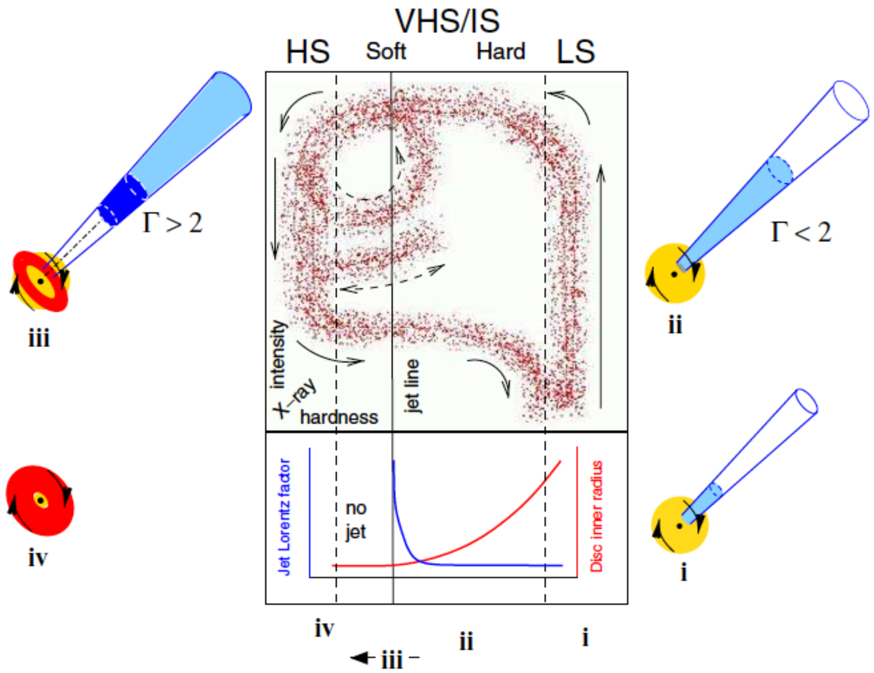

Fender et al. (2004)

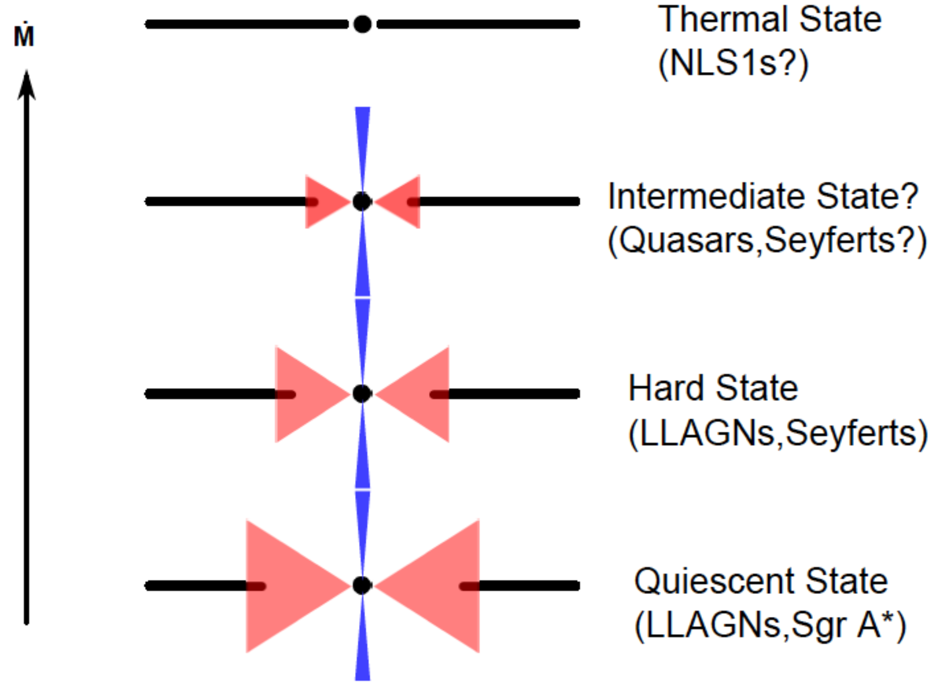

Yuan & Narayan (2014)

VLBI observations

- Morphologies: core & components - flux density, position angle, angular size, flux variability, proper motion and polarization

- Brightness temperature (Ghisellini et al. 1993)

$$T_{\rm B} = \frac{S_\nu \lambda^2}{2k\Omega_{\rm s}} = 1.77 \times 10^{12} (\frac{S_\nu}{\rm Jy})(\frac{\nu}{\rm GHz})^{-2}(\frac{\theta_d}{\rm mas})^{-2}, \theta_{\rm d} = \sqrt{\rm ab}$$

$$T_{\rm B}' = T_{\rm B}(1+z)/\delta$$

- Variability brightness temperature: (e.g. Yuan et al. 2008)

$$T_{\rm B,var} \gtrsim \frac{\Delta P_{\nu e}}{2\pi^2 k \nu^2 (\Delta t)^2} = \frac{2 D_{\rm L}^2 \Delta S_\nu}{(1+z)\pi k \nu^2 (\Delta t)^2}$$

$$T_{\rm B,var}' = T_{\rm B,var}/\delta^3$$

- Constraints on Doopler factor: equipartition brightness temperature Teq=5×10^{10} K (Readhead 1994); Inverse Compton limit Tb,int ~ 10^{12} K (Kellermann & Pauliny-Toth 1969)

Status of VLBI observations

- Radio-loud NLS1s: RXS J16290+4007, RXS J16333+4718, and B3 1702+457 (VLBA Gu & Chen 2010, Doi et al. 2011, JVN Doi et al. 2007), RX J0806.6+7248 (JVN Doi et al. 2007, VLBA Doi et al. 2011), B2 1111+32 (EVN, VLBA Chen & Gu in prep.).

- The gamma-ray NLS1s: compact at kpc scale, but resolved at pc scale (SBS 0846+513, PKS 1502+036 and PKS 2004-447, VLBA D'Ammando et al. 2012, Orienti et al. 2012,2015); SDSS J094857.31+002225.4 (VLBA Doi et al. 2006, Foschini et al. 2011, global e-VLBI Giroletti et al. 2011), 1H 0323+342 (VLBA Zhou et al. 2007), FBQS J1644+2619 (JVN Doi et al. 2007, VLBA Doi et al. 2011).

- In total, only about 11 RLNLS1s (out of 117) have published VLBI images before Gu et al. (2015, ApJS).

Results of our VLBA observations

(Gu et al. 2015, ApJS, 221, 3)

- The largest sample of 117 RLNLS1s (R>10) has been constructed by combining various samples available so far, which are mostly from our own work.
- Fourteen RLNLS1s with FIRST 1.4 GHz flux >10 mJy were observed with a total of 15 hours at 5 GHz using VLBA on Oct. and Nov., 2013.

- This is the first and largest systematic high resolution radio study of RLNLS1s.

- The jet physics: the jet formation in these accretion systems.
- The accretion – jet relation: early stages in both activities ?
- Feedback: jet – cloud interactions ?

Sample

Table 1: Sample of Radio-loud NLS1 Galaxies

Name	z	$f_{1.4\mathrm{GHz}}$ (mJy)	$f_{5\mathrm{GHz}}$ (mJy)	α	log R	a (arcsec)	LS (kpc)	r.s.
(1)	(2)	(3)	(4)	(5)	(6)	(7)	(8)	(9)
SDSS J081432.11+560956.6	0.509	69/60	43	-0.33	2.53	2.84	17.4	F
SDSS J085001.17+462600.5	0.523	21/16			2.23	1.26	7.8	S
SDSS J090227.16+044309.6	0.532	153/157	106	-0.30	3.02	1.00	6.3	F
SDSS J095317.09+283601.5	0.657	45/43			2.71	1.95	13.6	S[a]
SDSS J103727.45+003635.6	0.595	27/28			2.66	1.16	7.7	F[a]
SDSS J104732.68+472532.1	0.798	734/789	404	-0.51	3.87	1.16	8.7	S
SDSS J111005.03+365336.3	0.630	19/23			2.97	2.08	14.2	S
SDSS J113824.54+365327.1	0.356	13/12			2.34	0.43	2.1	S
SDSS J124634.65+023809.0	0.362	37/36	46	0.17	2.38	1.12	5.6	F
SDSS J130522.75+511640.3	0.785	84/87	46	-0.50	2.34	1.34	10.0	S
SDSS J142114.05+282452.8	0.538	48.7/45.4	40	-0.15	2.31	1.28	8.1	F
SDSS J144318.56+472556.7	0.703	165/166	72	-0.67	3.07	1.18	8.4	S
SDSS J154817.92+351128.0	0.478	141/141	107	-0.22	2.84	0.51	3.0	F
SDSS J163401.94+480940.2	0.494	8/14			2.31	1.15	6.9	F

Notes. — Col. (1): source name; Col. (2) redshift; Col. (3): the FIRST and NVSS flux densities at 1.4 GHz (in the format of FIRST/NVSS); Col. (4): the flux density at 5 GHz from the literature; Col. (5): the spectral index between 1.4 and 5 GHz when available ($f_\nu \propto \nu^\alpha$); Col. (6): the radio loudness defined as $f_\nu(1.4\mathrm{GHz})/f_\nu(4400\mathrm{\AA})$; Col. (7): the major axis from FIRST; Col. (8): the upper limit on the source linear size calculated from the FIRST major axis; Col. (9): the radio spectrum based on low-resolution NED data (see Section 4.3): F - flat spectrum, S - steep spectrum, [a] - uncertain (see text for details).

Morphology

- Generally compact: seven sources show compact core only, and other seven objects have core-jet structure.

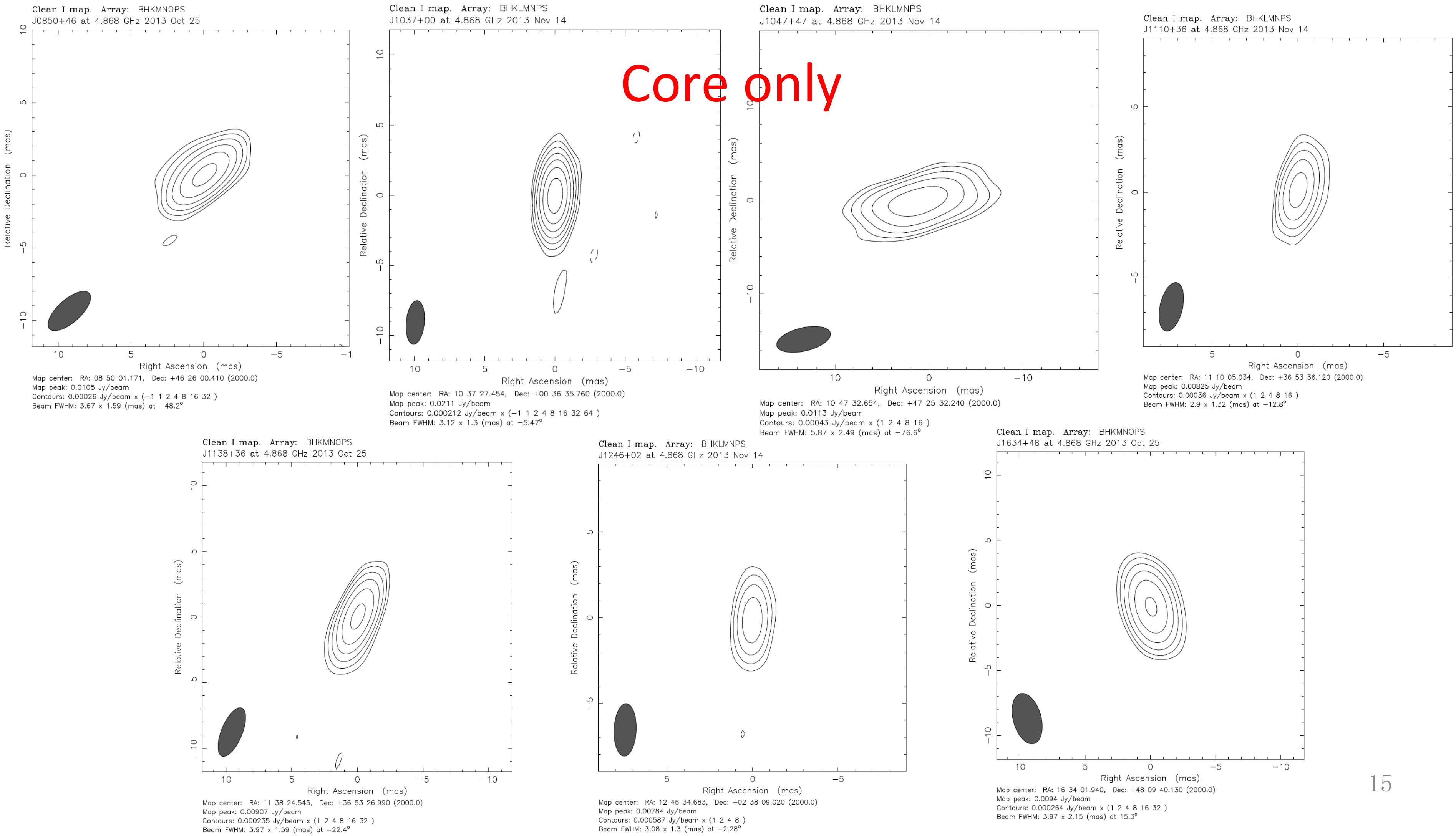

Core-jet

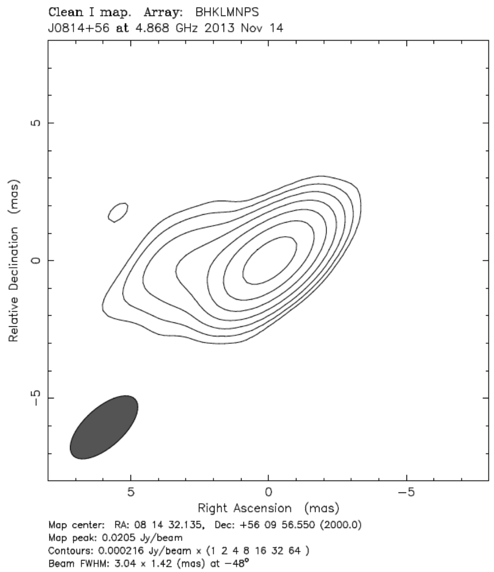
Clean I map. Array: BHKLMNPS
J0814+56 at 4.868 GHz 2013 Nov 14
Relative Declination (mas)
Right Ascension (mas)
Map center: RA: 08 14 32.135, Dec: +56 09 56.550 (2000.0)
Map peak: 0.0205 Jy/beam
Contours: 0.000216 Jy/beam x (1 2 4 8 16 32 64)
Beam FWHM: 3.04 x 1.42 (mas) at −48°

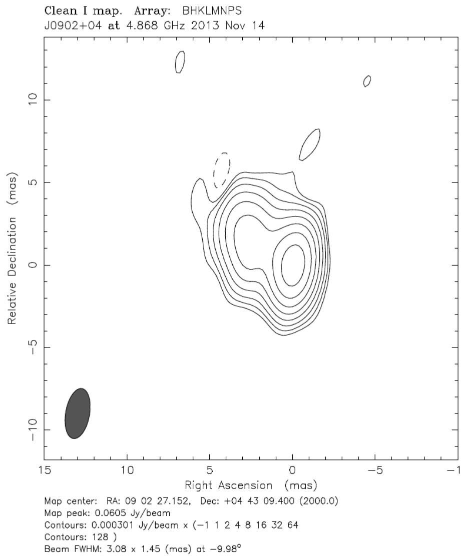
Clean I map. Array: BHKLMNPS
J0902+04 at 4.868 GHz 2013 Nov 14
Relative Declination (mas)
Right Ascension (mas)
Map center: RA: 09 02 27.152, Dec: +04 43 09.400 (2000.0)
Map peak: 0.0605 Jy/beam
Contours: 0.000301 Jy/beam x (−1 1 2 4 8 16 32 64
Contours: 128)
Beam FWHM: 3.08 x 1.45 (mas) at −9.98°

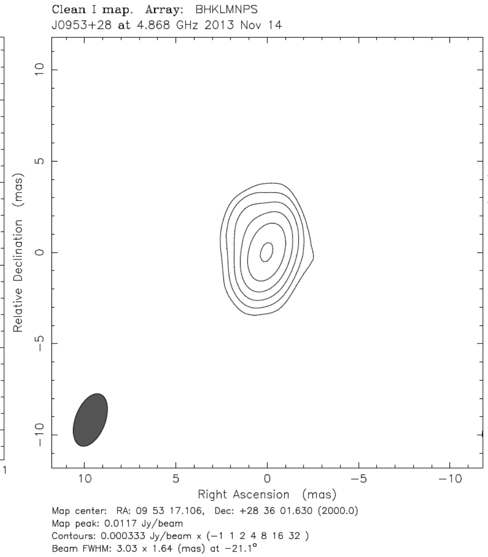
Clean I map. Array: BHKLMNPS
J0953+28 at 4.868 GHz 2013 Nov 14
Relative Declination (mas)
Right Ascension (mas)
Map center: RA: 09 53 17.106, Dec: +28 36 01.630 (2000.0)
Map peak: 0.0117 Jy/beam
Contours: 0.000333 Jy/beam x (−1 1 2 4 8 16 32)
Beam FWHM: 3.03 x 1.64 (mas) at −21.1°

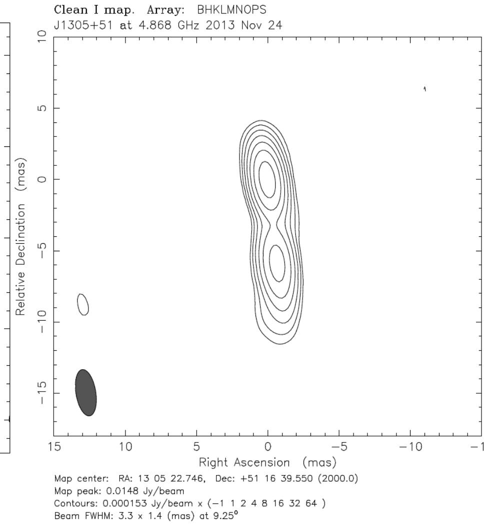
Clean I map. Array: BHKLMNOPS
J1305+51 at 4.868 GHz 2013 Nov 24
Relative Declination (mas)
Right Ascension (mas)
Map center: RA: 13 05 22.746, Dec: +51 16 39.550 (2000.0)
Map peak: 0.0148 Jy/beam
Contours: 0.000153 Jy/beam x (−1 1 2 4 8 16 32 64)
Beam FWHM: 3.3 x 1.4 (mas) at 9.25°

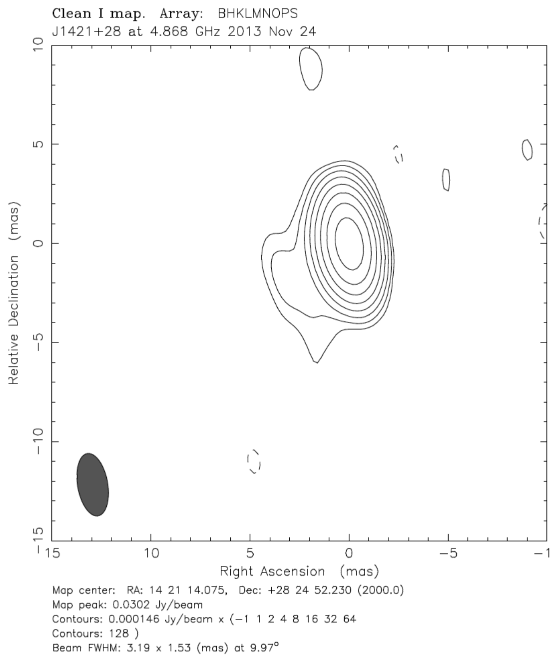
Clean I map. Array: BHKLMNOPS
J1421+28 at 4.868 GHz 2013 Nov 24
Relative Declination (mas)
Right Ascension (mas)
Map center: RA: 14 21 14.075, Dec: +28 24 52.230 (2000.0)
Map peak: 0.0302 Jy/beam
Contours: 0.000146 Jy/beam x (−1 1 2 4 8 16 32 64
Contours: 128)
Beam FWHM: 3.19 x 1.53 (mas) at 9.97°

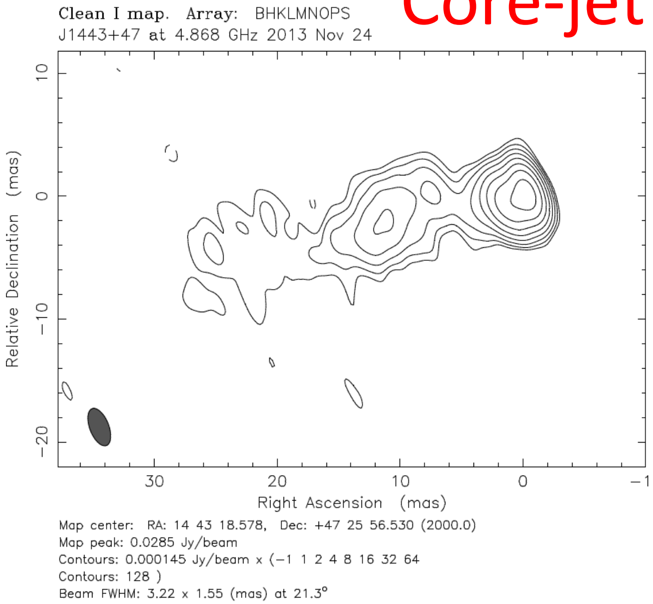
Clean I map. Array: BHKLMNOPS
J1443+47 at 4.868 GHz 2013 Nov 24
Relative Declination (mas)
Right Ascension (mas)
Map center: RA: 14 43 18.578, Dec: +47 25 56.530 (2000.0)
Map peak: 0.0285 Jy/beam
Contours: 0.000145 Jy/beam x (−1 1 2 4 8 16 32 64
Contours: 128)
Beam FWHM: 3.22 x 1.55 (mas) at 21.3°

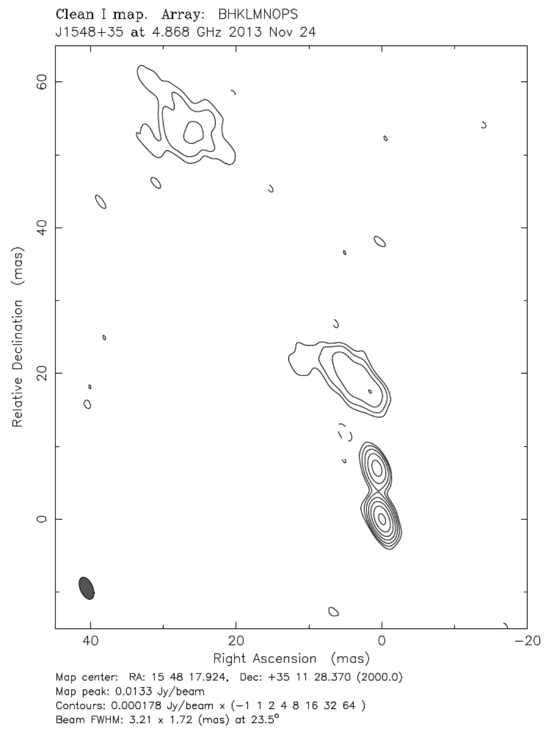
Clean I map. Array: BHKLMNOPS
J1548+35 at 4.868 GHz 2013 Nov 24
Relative Declination (mas)
Right Ascension (mas)
Map center: RA: 15 48 17.924, Dec: +35 11 28.370 (2000.0)
Map peak: 0.0133 Jy/beam
Contours: 0.000178 Jy/beam x (−1 1 2 4 8 16 32 64)
Beam FWHM: 3.21 x 1.72 (mas) at 23.5°

Radio spectra

- From the multi-band radio data, seven sources show flat or even inverted spectra, while steep spectra are found in rest objects.

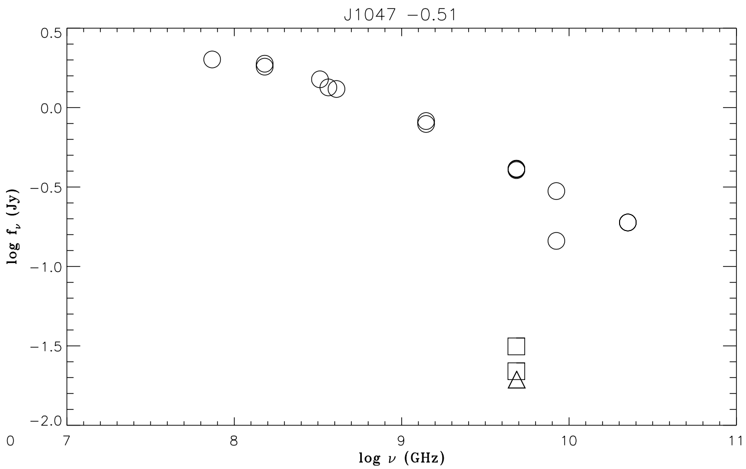

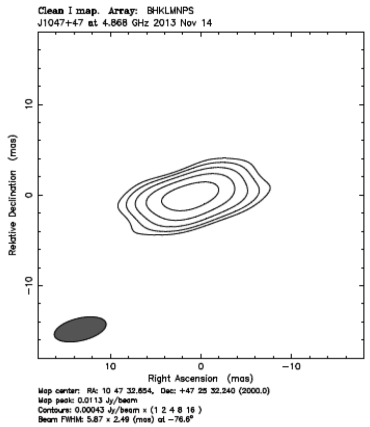

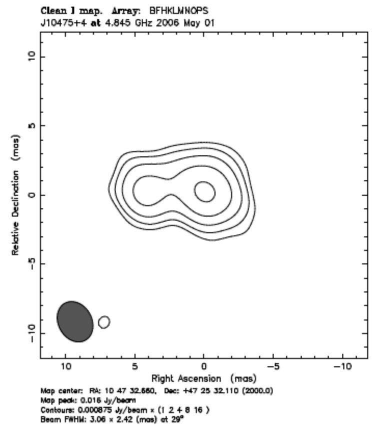

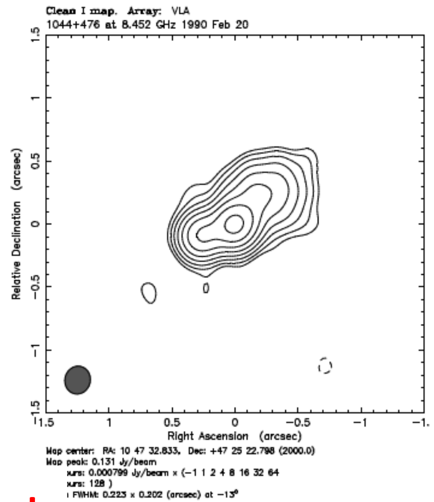

Steep radio spectrum – resemble to Compact Steep Spectrum sources

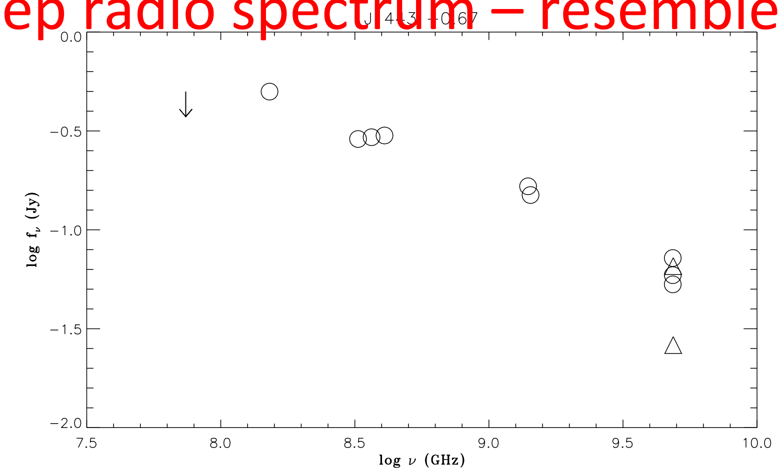

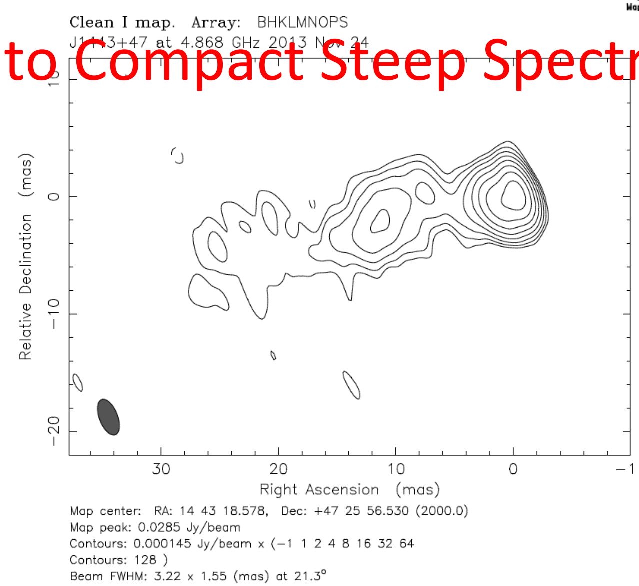

- Fermi detected ? (Foschini 2011): SDSS J124634.65+023809.0 (TS=15)
- Core only, different from others

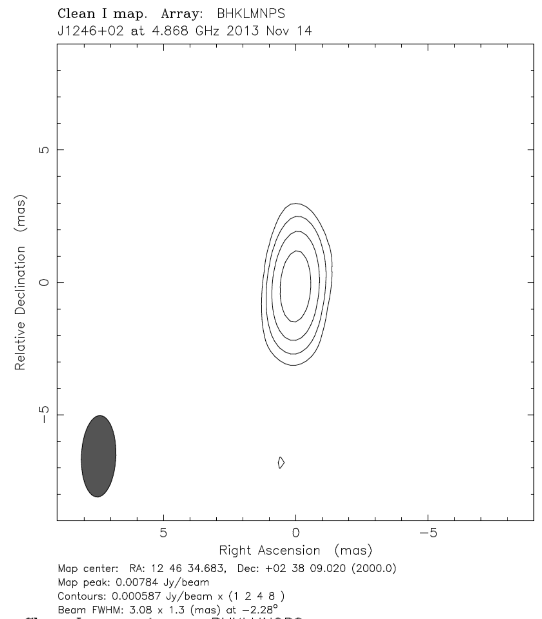

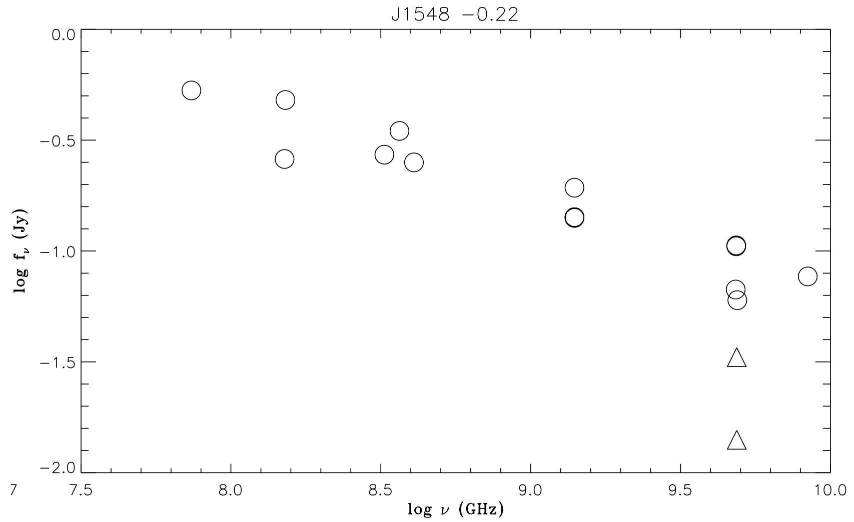

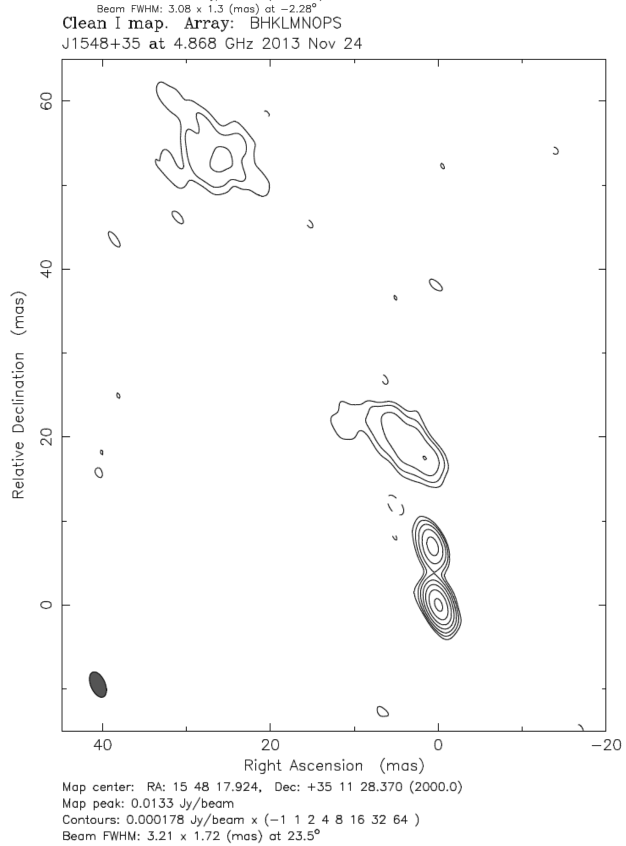

Flat radio spectrum – blazar like

(see also Orienti et al. 2015 for VLBA images)

Brightness temperature

- The core brightness temperature ranges from $10^{8.4}$ to $10^{11.4}$ K with a median value of $10^{10.1}$ K.
- The radio emission is from non-thermal jets, and the beaming effect is generally not significant.
- Typical blazars have 10^{11} - 10^{13} K with a median value near 10^{12} K (Kovalev et al. 2005, 2009).
- The bulk jet speed may likely be low in our sources (see also Angelakis et al. 2015, Richards & Lister 2015).

Kovalev et al. 2009

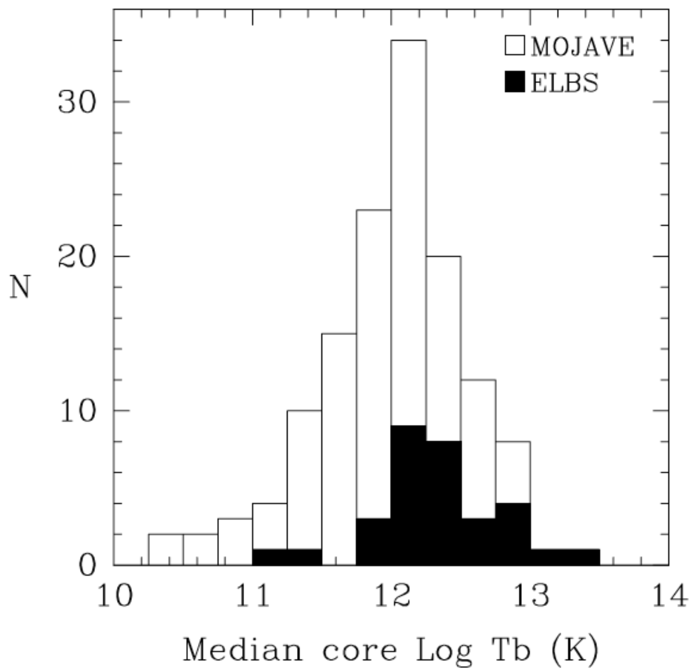

Comparisons to typical CSSs: VLBI morphology

- Most high-power CSSs show double or triple morphologies (O'Dea 1998, Dallacasa et al. 2013)

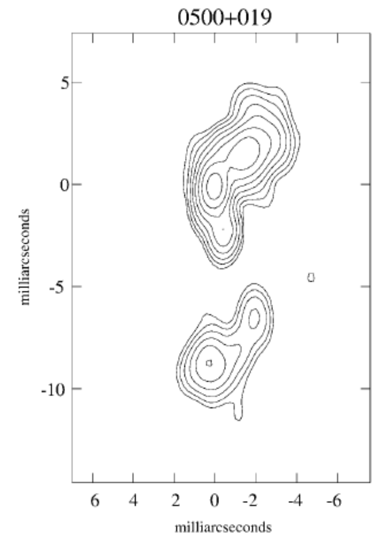

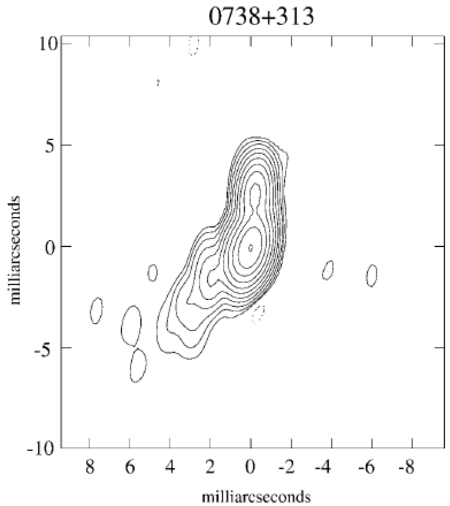

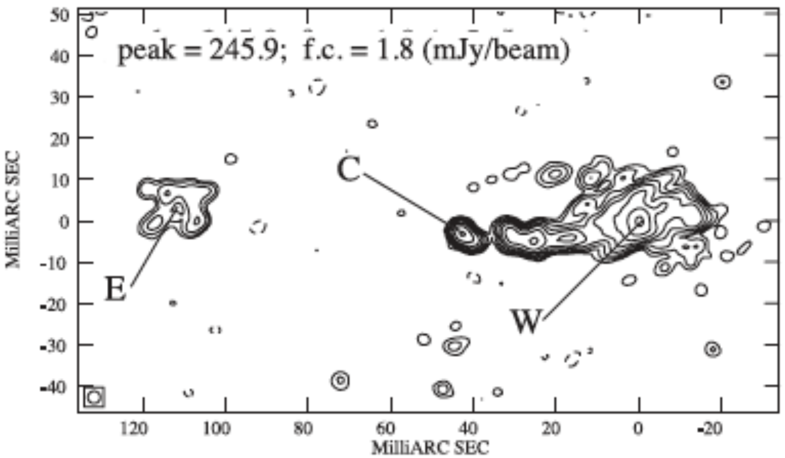

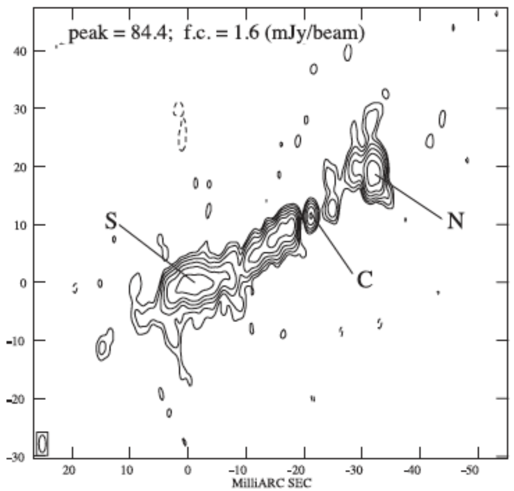

Core and core-jet in low-power CSSs

- The compact core only, or core-jet structure have been detected in relatively low-power CSS sources (Kunert-Bajraszewska et al. 2006; Kunert-Bajraszewska & Marecki 2007)

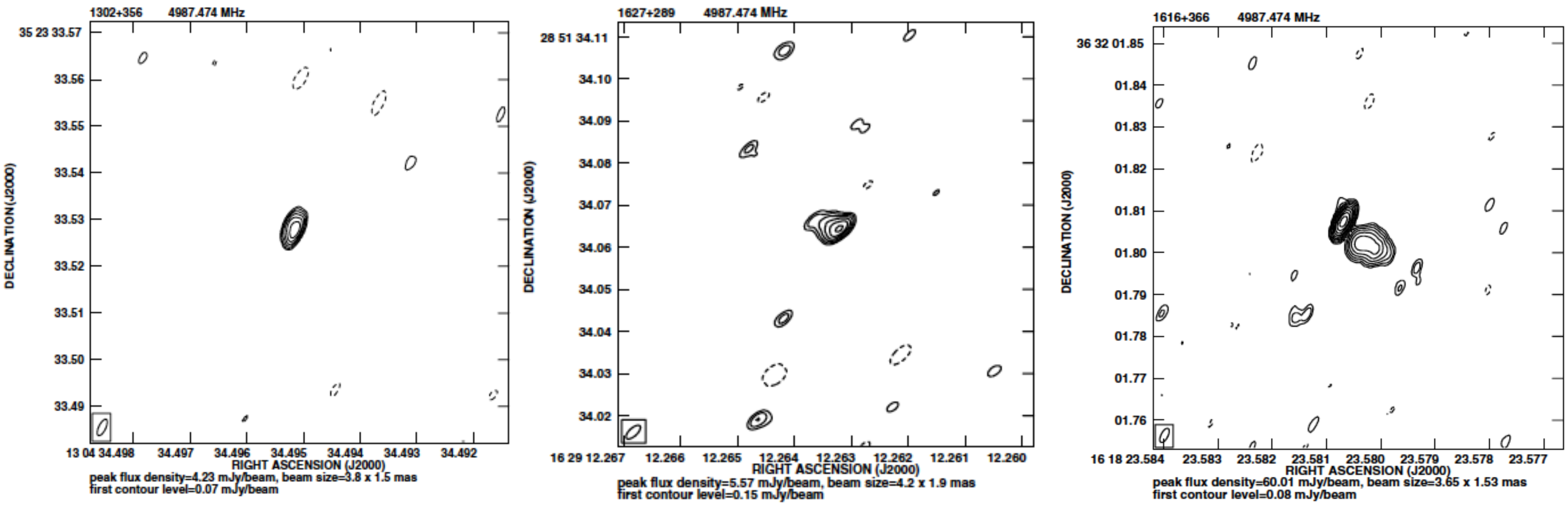

Evolution

- Our sources occupy the space below the main evolutionary path of radio objects (An & Baan 2012).
- However, the difference is that our sources have small black hole mass and high accretion rate.

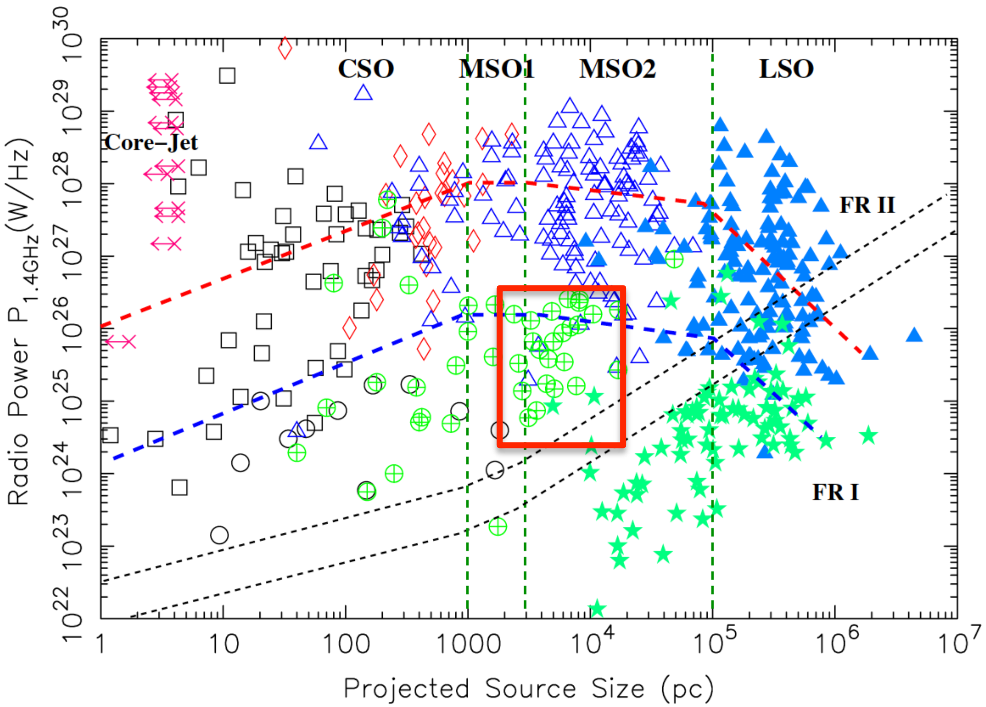

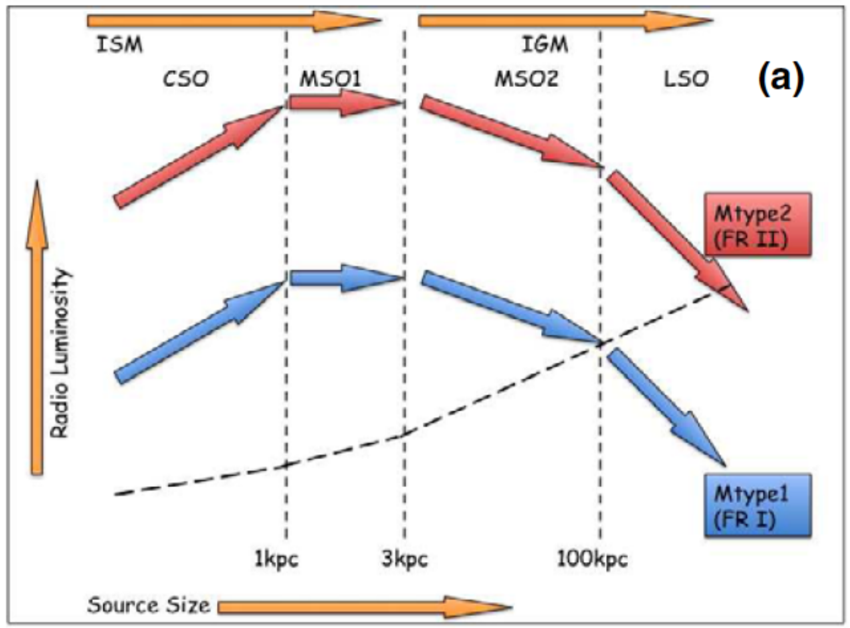

Scenario： low jet speed

- a) The outflows/jets accelerated from the hot corona above the disk by the magnetic field and radiation force, with high mass loss rate but low speed (Cao 2014).

- The M_{BH} - Γ correlation: the faster moving jets are magnetically accelerated by the magnetic fields threading the horizon of more rapidly rotating black holes (Chai, Cao & Gu 2012).
- b) The low jet speed could be due to the low spin, supported by low/intermediate average spins (a < 0.84) from composite broad Fe K line (Liu et al. 2015).

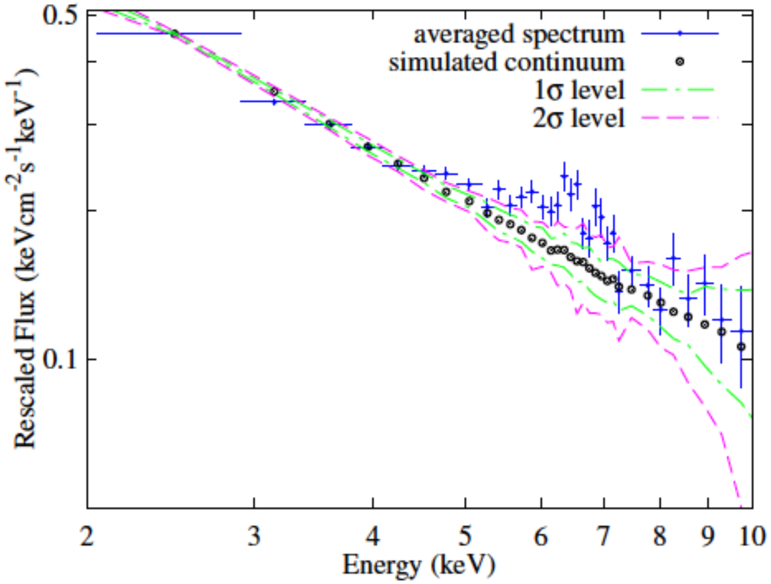

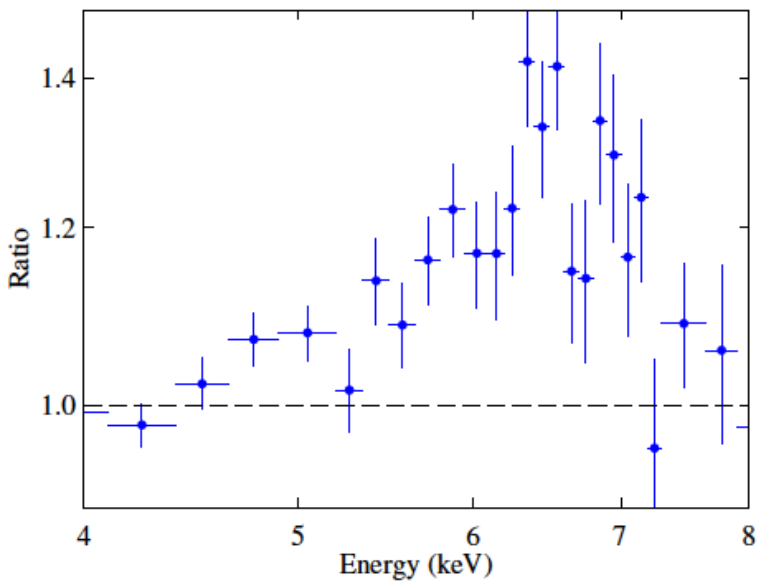

Ongoing work (I)

Gu et al. in prep.

- The additional 19 RLNLS1s with FIRST flux density >=6 mJy have been observed with VLBA in a total of 24 hours in Nov. and Dec. 2014, yielding the biggest VLBI sample of 33 sources.
- Five core-jet, and fourteen core-only; low brightness temperature compared to blazars; steep-spectrum and flat-spectrum sources.

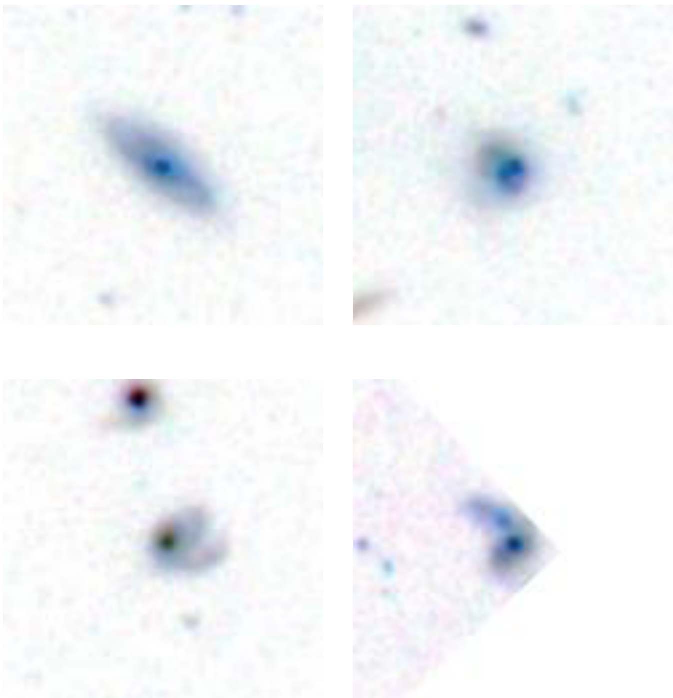

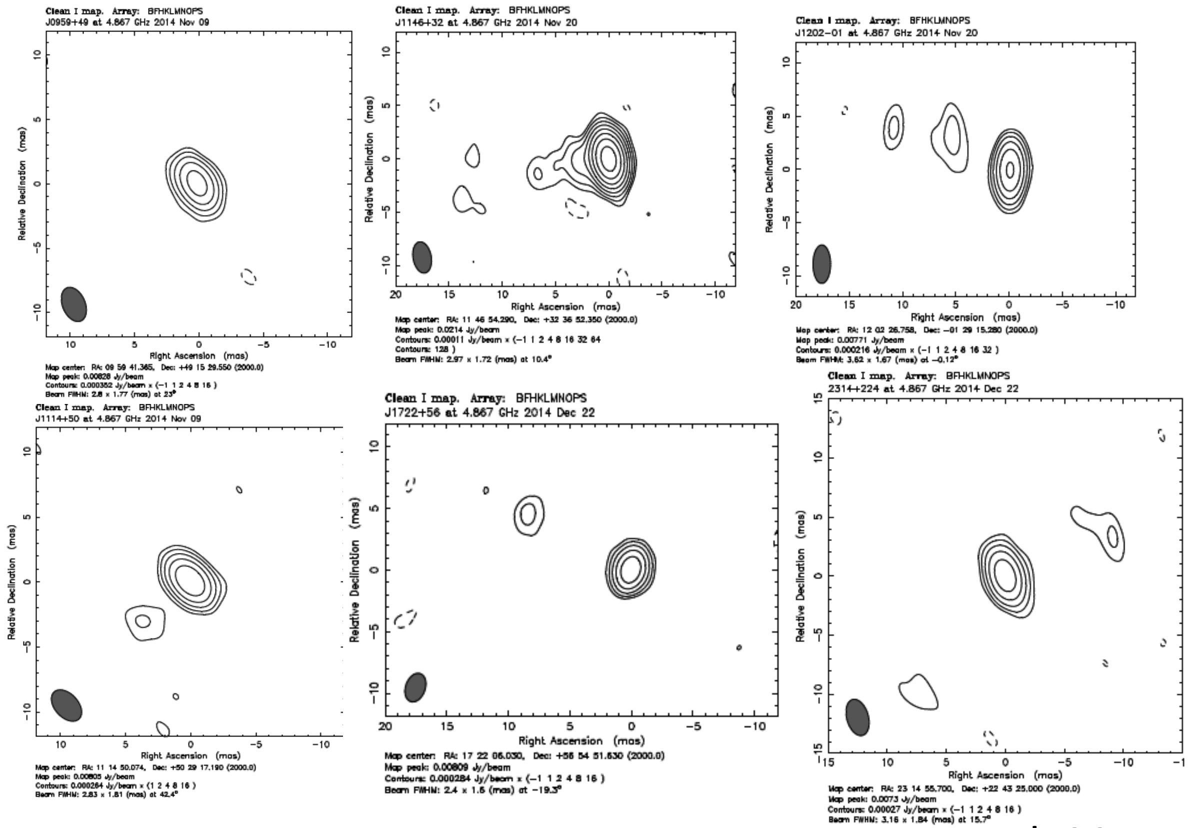

Komossa et al. 2015

Ongoing work (II)

- To constrain the jet bulk velocity, 10 sources with core-jet structure have been observed with VLBA for 14 hours in Apr. 2016, and Oct. 2015, to detect the jet proper motion.

Table 1: Sample of Radio-loud NLS1 Galaxies

Name (1)	z (2)	$f_{5\mathrm{GHz}}$ (mJy) (3)	archive (4)	*Fermi* (5)
SDSS J081432.11+560956.6	0.509	43	2006-May,2013-Nov.,2014-May	No
SBS 0846+513	0.584	161	1995-Mar.,1996-Jan.,Dec.,2004-Mar.,2014-May	Yes
SDSS J090227.16+044309.6	0.532	106	2013-Nov.	No
SDSS J094857.31+002225.4	0.585	295	2000-Apr.,2013-Mar.,2014-Jan.	Yes
SDSS J104732.68+472532.1	0.798	404	2006-May,2013-Nov.	No
SDSS J130522.75+511640.3	0.785	46	2013-Nov.	No
SDSS J142114.05+282452.8	0.538	40	2013-Nov.	No
SDSS J144318.56+472556.7	0.703	72	2013-Nov.	No
PKS 1502+036	0.409	859	2001-Oct.,2006-Jun.,2013-Jun.,2014-Jan.,Jul.,Aug.	Yes
SDSS J154817.92+351128.0	0.478	107	2013-Jan.,2013-Nov.	No

Notes. — Col. (1): source name; Col. (2) redshift; Col. (3): the flux density at 5 GHz; Col. (4): the previous VLBA 5 GHz observations; Col. (5): whether the source is detected by *Fermi* LAT.

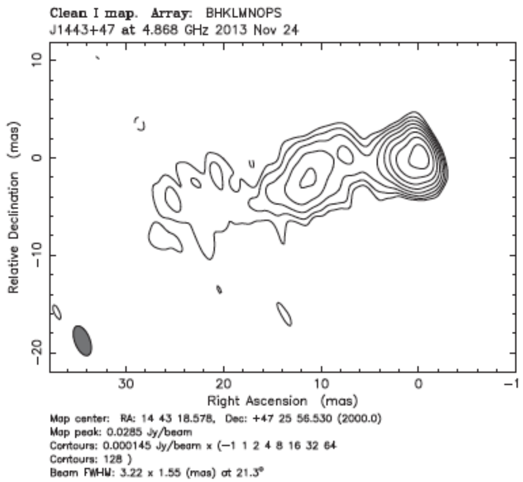

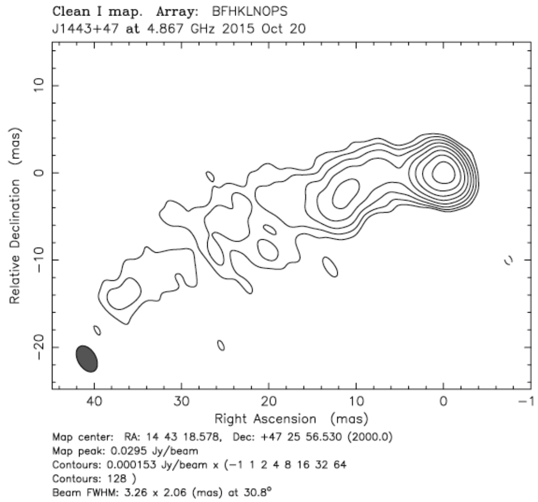

Ongoing work (III)

SDSS J1433+4725: a gamma-ray detected NLS1 galaxy with CSS-like property

Abstract:

SDSS J1443+4725 (z=0.703) is a radio-loud narrow line Seyfert 1 galaxy (NLS1) with radio properties similar to compact steep spectrum (CSS) sources. We recently found gamma-ray emission at high significance from Fermi/LAT. Its uniqueness makes it precious in studying the accretion process, jet activity and high energy emission. Our previous VLBA 5 GHz observation shows a likely core-jet structure with seven components in central regions and diffuse extended emission at outer regions. As continuation of our systematical study on the jet properties of radio-loud NLS1s, we propose multi-frequency polarimetry observations on SDSS J1443+4725 with VLBA at 2.3, 5.0, 8.4, 15.3, and 22 GHz, for a total observing time of 10.5 hours. We aim to study the jet physics in details, including identification of radio core, core-shift effect, variability, proper motion, and polarization. All these information will be crucial in understanding the gamma-ray emission, in terms of its origin (jets or/and core), and the role of beaming effect etc..

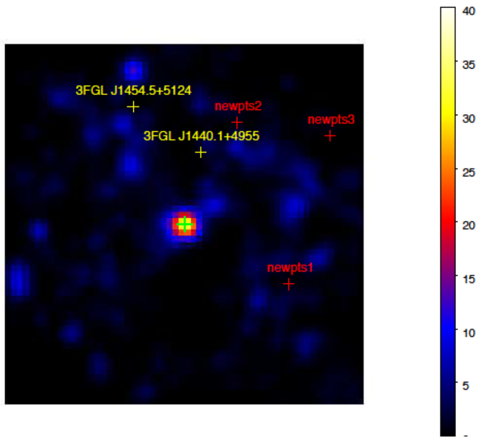

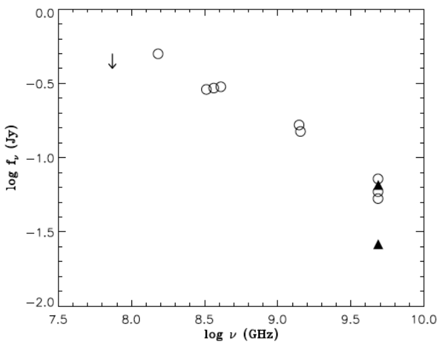

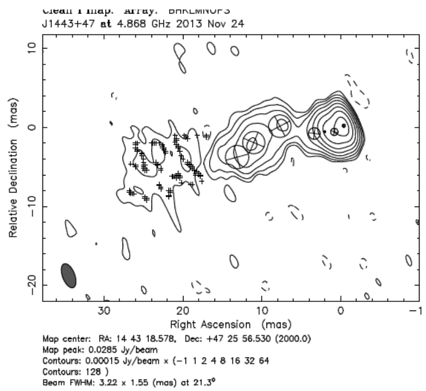

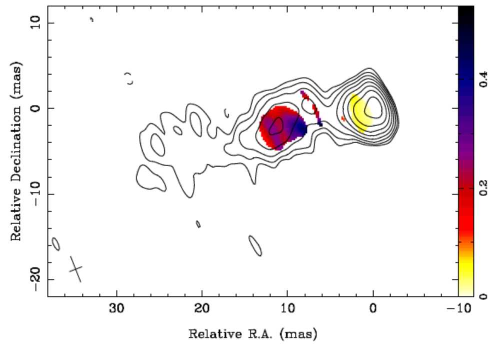

Liao et al. arXiv: 1510.05584

Summary

- Powerful jets may present in systems with small M_{BH} and high accretion rate, e.g. NLS1s.
- The jet properties of radio-loud NLS1s are diverse on mas scale, in terms of the morphology and spectral shape.
- The jet speed in these sources is likely low, which is due to either the jet acceleration by the magnetic field and radiation force, or low spin in BZ mechanism.
- The slow jet speed or mildly relativistic jet, in combination with the low kinetic/radio power, could be responsible for the compact VLBA radio structure in most sources.

Thanks for your attention !

Polarization

- The higher fractional polarization in jets: the strong Faraday rotation in nuclei region due to the high plasma density, and/or depolarization due to the complex core structure.
- The gradient of fractional polarization along the direction perpendicular to the jet elongation : the jet-ISM interaction at the locations of high fractional polarization because of the jet bulk motion.